Electronic Supplementary Material (ESI) for Sustainable Energy & Fuels.

Supporting Information

Thermally integrated photoelectrochemical devices with perovskite/silicon tandem solar cells: a modular approach for scalable direct water splitting

Angela R. A. Maragno[a], Adina Morozan[b], Jennifer Fize[b], Michel Pellat[c], Vincent Artero[b,*], Sophie Charton[a,*], Muriel Matheron[d,‡,*]

[a] CEA, DES, ISEC, DMRC, Univ. Montpellier, Marcoule, France

[b] Univ. Grenoble Alpes, CNRS, CEA, IRIG, Laboratoire de Chimie et Biologie des Métaux, 38000 Grenoble, France

[c] Univ. Grenoble Alpes, CEA, LITEN, DTNM, 38000 Grenoble, France

[d] Univ. Grenoble Alpes, CEA, LITEN, Campus INES, 73375 Le Bourget du Lac, France

[*] Lead contacts

[‡] Present address: Univ. Grenoble Alpes, CEA, LITEN, DTCH, 38000 Grenoble, France

IPEC cell and module components

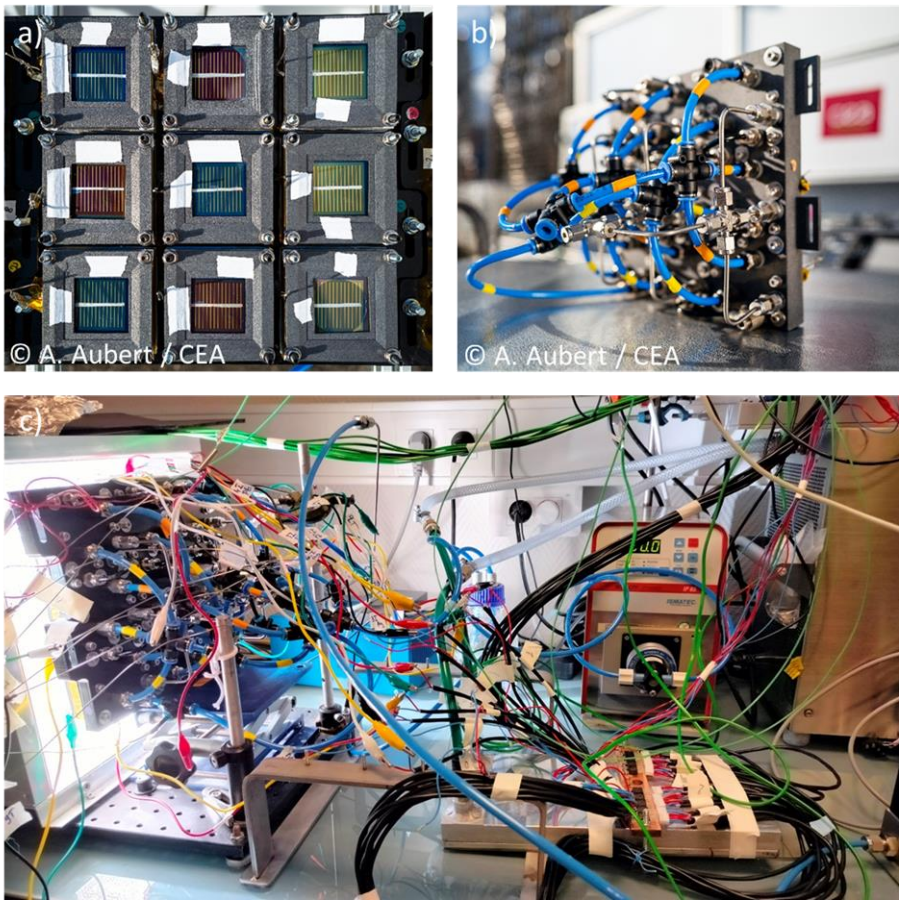

Figure S1 – a) Front side (illuminated side) of an IPEC module. Tandem solar cells have different colours due to changes in perovskite and PTAA thickness. b) Back side of the IPEC module showing the water inlet circuit (plastic tubes) and

hydrogen outlet circuit (metal tubes). c) Temperature measurement set-up for the 1 sun illuminated IPEC module through multiple temperature sensors (from Figure 4).

Table S1 – Components of the IPEC cell and module

Component	Specific features
Anodic box	Polyoxymethylene (POM), 7 × 7 cm^2 (cell), 21 × 22 cm^2 (module)
Anodic plate	Current collecting plate with flow channels, 3D-printed polypropylene (PP): active flow area of 3.5 × 3.5 cm^2, 6 machined serpentine channels of 1 mm width Electrically conductive coating: sputtered bilayer of Cr/Au (5 nm/200 nm)
Pt wire	4 cm length, 1 mm diam. (Alfa Aesar), ensures electrical contact between anode and solar cell
Pt/Ti grid	Platinum-coated titanium grid (254 µm thick, 3.5 × 3.5 cm^2, FuelCellStore)
Membrane Electrode Assembly	Anode catalyst: 5.7 mg cm^{-2} Ir black (Alfa Aesar) Nafion NRE-212 membrane (50 µm thick, Alfa Aesar) Gas diffusion cathode: 0.5 mg·cm^{-2} 60% Pt-Vulcan/carbon cloth (FuelCellStore) Active surface area of 3.5 × 3.5 cm^2
Gaskets	Silicon (GETELEC) of thickness: 300 µm anode side, 200 µm cathode side, 1 mm between anodic plate and anodic box
Cathodic plate	Current collecting plate with flow channels, 3D-printed 316L stainless steel: external area 6.5 × 6.5 cm^2, active flow area of 3.5 × 3.5 cm^2, flow channels consisting of 1 mm width-cubic pins, internal heat exchanger with 13 machined flow channels of 2.3 mm diameter
In sheet	Indium film 100 µm-thick (Chimie Tech Services), ensures electrical contact between cathodic box and solar cell backside
Solar cell	Perovskite/silicon tandem solar cell: 3 × 3 cm^2 on a 5 × 5 cm^2 substrate, metallization shading of ca. 15 % of the illuminated surface, 7.6 cm^2 active area
Mask	Polyamide 11 (PA11): external area 6.5 × 6.5 cm^2, internal area 10.24 cm^2

Determination of solar cells active area

Active area is defined as the area where all layers of the solar cells are stacked, taking into account the shading from opaque metallization (evaporated gold and additional metal ribbon) deposited on the front side. We used ImageJ software and a contrast determination method to determine A_{stack}, the area where all layers are stacked (in average, 9.0 cm^2), from which we subtracted A_{shaded}, the average area occupied by metallization (in average, 1.4 cm^2).

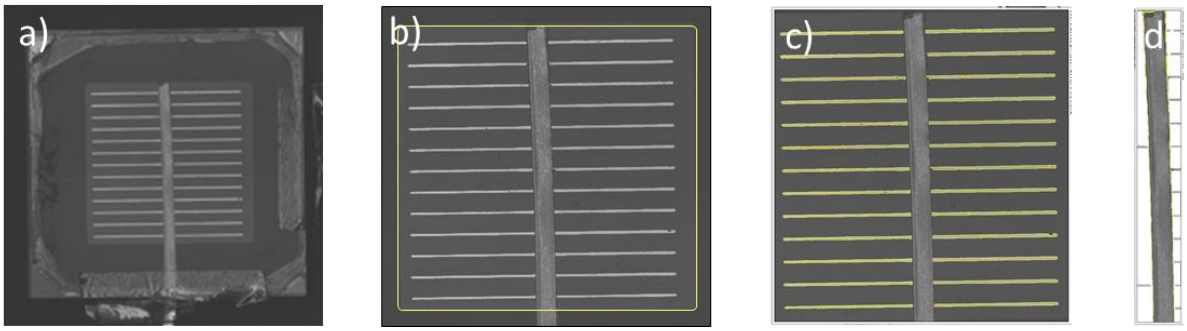

Figure S2 – Determination of the active area of a perovskite/silicon tandem solar cell. a) Initial image of the solar cell's front side, showing the 5 × 5 cm² substrate with the 3 × 3 cm² central zone where all layers are present. This central zone is defined by the 3 × 3 cm² front side ITO hard mask. b) In yellow, the area selection corresponding to A_{stack}, as determined with ImageJ. c) Within this central zone, in yellow, the area selection correponding to gold metallization. d) In yellow, the area corresponding to the metal ribbon. A_{shaded} is determined summing the areas from c) and d).

Table S2 – Determination of perovskite/silicon tandem solar cells active area.

	A_{stack} (cm²)	**A_{shaded} (cm²)**	**Active area ($A_{stack} - A_{shaded}$) (cm²)**	**% shaded (A_{shaded}/A_{stack})**
Cell 1	9.0	1.6	7.5	17.2
Cell 2	9.1	1.4	7.7	15.7
Cell 3	9.0	1.2	7.8	13.4
Average	**9.0**	**1.4**	**7.6**	**15.4**

Pictures of the IPEC modules in the outdoor experiment

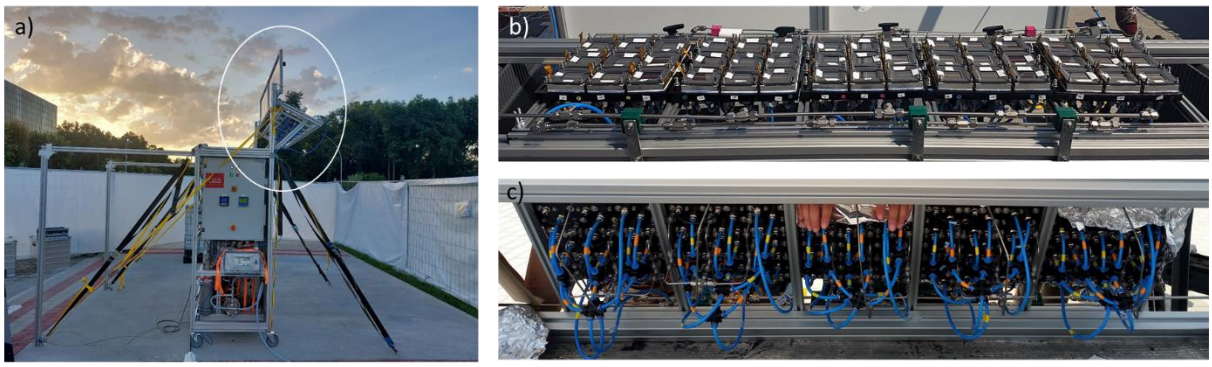

Figure S3 – a) IPEC modules (circled) integrated into the autonomous device dedicated to the production of green methane at JRC in Ispra during the 72 hour demonstration outdoors (31). b) Front side and c) back side of the five IPEC modules aged outdoor.

Determination of the correction factor for the horizontal irradiance

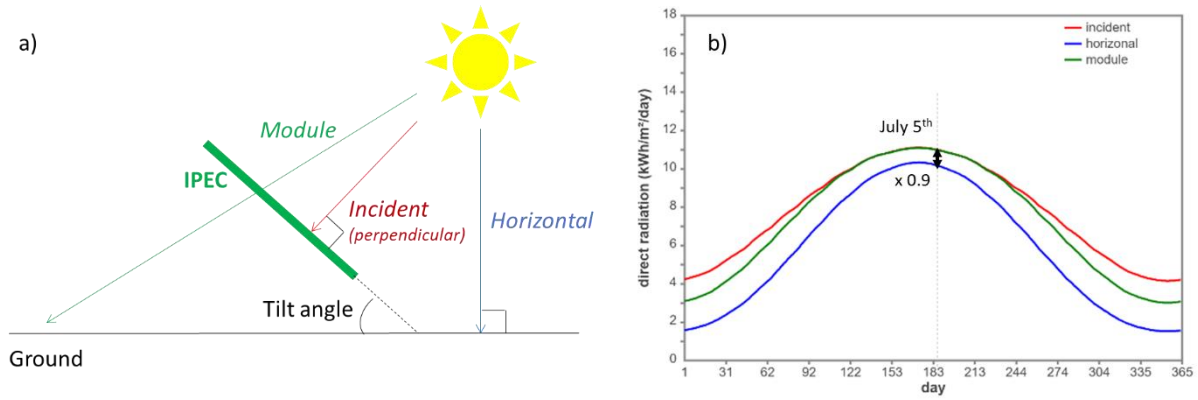

Figure S4 – Direct radiation striking a tilted plane. a) Sheme of the IPEC modules, tilted 25° against the horizontal. b) Calculated direct radiation on the IPEC modules (in green), on the horizontal plane (in blue), and on the plane always perpendicular to the sun thanks to a light tracker. The latitude was 45° N. Day on the abscissa is the number of days since January 1st. The ratio of irradiances used to correct the GHI for STH* calculation is 0.9. Figure and calculations adapted from (55).

Typical maximum power point voltages of perovskite/silicon solar cells under 1 sun

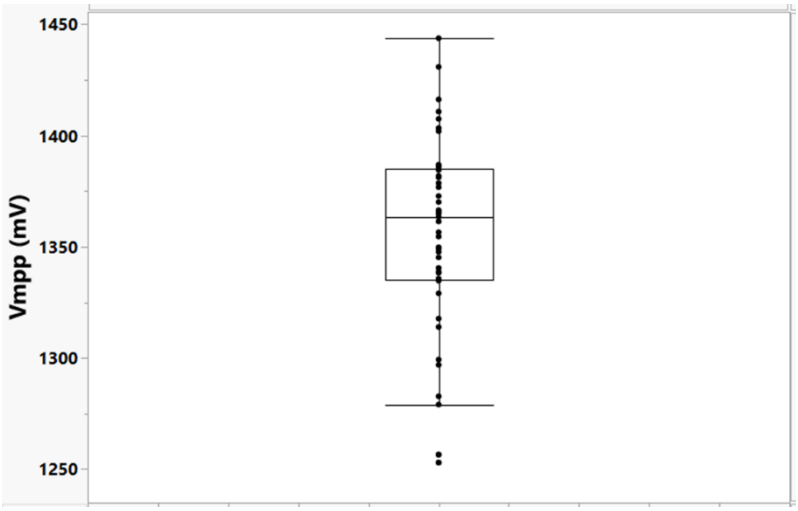

Figure S5 – Typical voltages reached at the maximum power point for the perovskite/silicon tandem solar cells under 1 sun (minimum value: 1253 mV, maximum value : 1444 mV, median value: 1364 mV).

Structure of the 3D-printed cathode with the heat exchanger

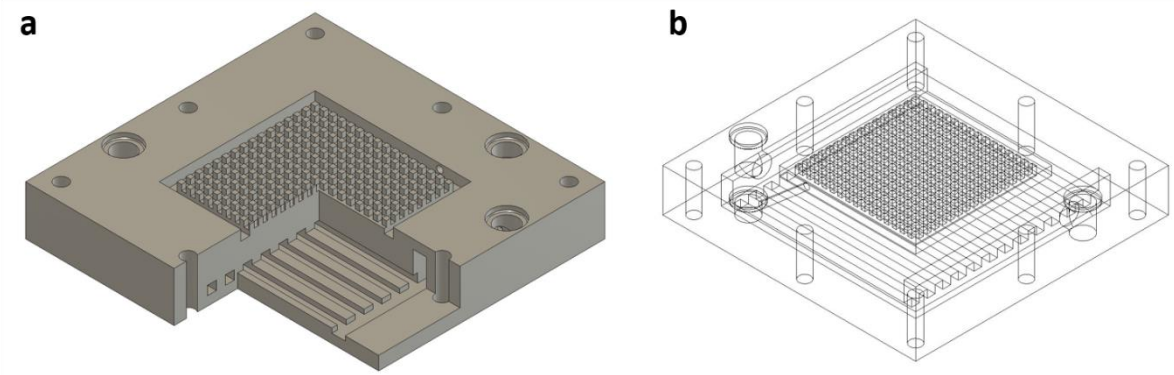

Figure S6 – Design of the 3D-printed metallic flow plate showing the heat exchanger channels and the central rough conductive surface.

Faradic efficiency during various IPEC cell performance tests

Table S3 – Faradic efficiency in IPEC cells under 1 sun illumination, during long and short operational periods. The average value of FE is used for the STH efficiency calculations.

	Faradic efficiency (FE) (%)
IPEC cell (Table 1)	74
Cycle 1 (Table 2)	80
Cycle 2 (Table 2)	76
Cycle 3 (Table 2)	70
Cycle 1 (Table S4)	75
Cycle 2 (Table S4)	68
Cycle 3 (Table S4)	71
Average	**74**

Influence of heat exchanger on IPEC cell performance

Table S4 – IPEC cell performance under cycles of continuous 1 sun illumination, without or with heat exchanger. Active area 7.3 cm² in the case without heat exchanger.

Cycle	V_{op} (V)	Average I_{op} (mA)	t (h)	Vol. H_2 (L)	STH (%)	STH* (%)
without heat exchanger						
1	1.44	69	5	0.06	4.6	4.6
2		76	8	0.09	3.8	3.8
3		65	10	0.07	2.5	2.5
with heat exchanger						
1	From 1.44 to 1.5	60	8	0.16	7.3	7.3
2		57	8	0.14	6.6	6.4
3		45	8	0.12	6.9	5.1

Estimation of STH efficiency from I(V) curves of perovskite/silicon tandem solar cells

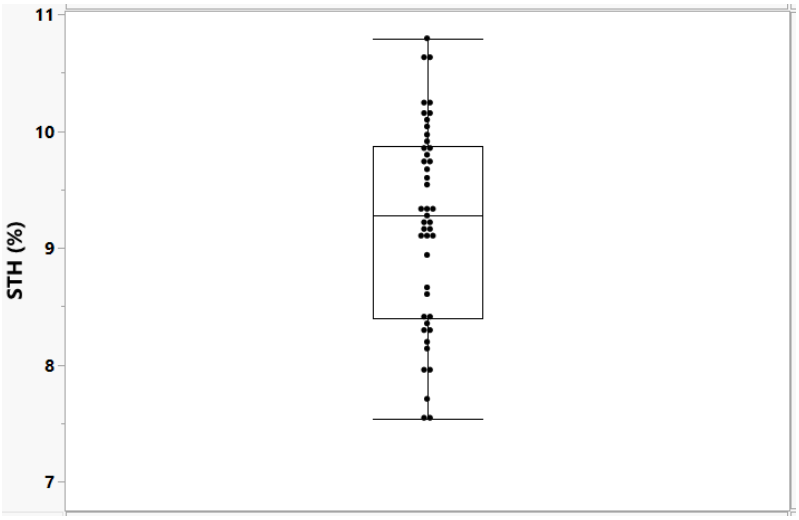

Figure S7 – Estimated initial STH efficiency for the forty five IPEC cells from the current densities of the solar cells (disconnected from the PEM electrolyser) measured at 1.45 V under 1 sun. The Faradaic efficiency was taken at 74 %. STH range from 7.5 up to 10.8 %.

IPEC cell stability under light/dark cycles (repeated)

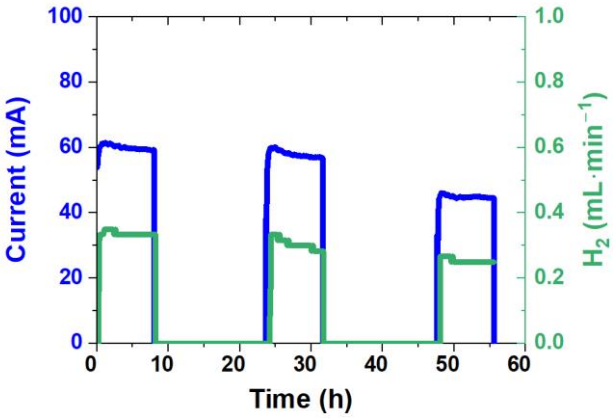

Figure S8 – IPEC cell stability under light / dark cycles (repeated experiment from Figure 3). Operating current (in blue) and hydrogen flow rate (in green).

Operating current of the nine IPEC cells from the IPEC module

Table S5 – Operating currents of the nine IPEC cells comprising the IPEC module. The corresponding STH efficiencies were calculated with a Faradaic efficiency of 74 %. Values of operating currents are given at the beginning and at the end of the 6 h stability run under continuous illumination from Figure 4.

	Initial		**Final**	
Solar cell	**I_{op} (mA)**	**STH (%)**	**I_{op} (mA)**	**STH (%)**
1	36	4.3	35	4.2
2	45	5.4	34	4.1
3	26	3.1	30	3.6
4	57	6.8	44	5.3
5	30	3.6	6	0.7
6	33	4.0	36	4.3
7	46	5.5	25	3.0
8	24	2.9	20	2.4
9	29	3.5	26	3.1
Average	**36**	**4.3**	**28**	**3.4**

Impact of variations in perovskite and p-layer thicknesses on performance

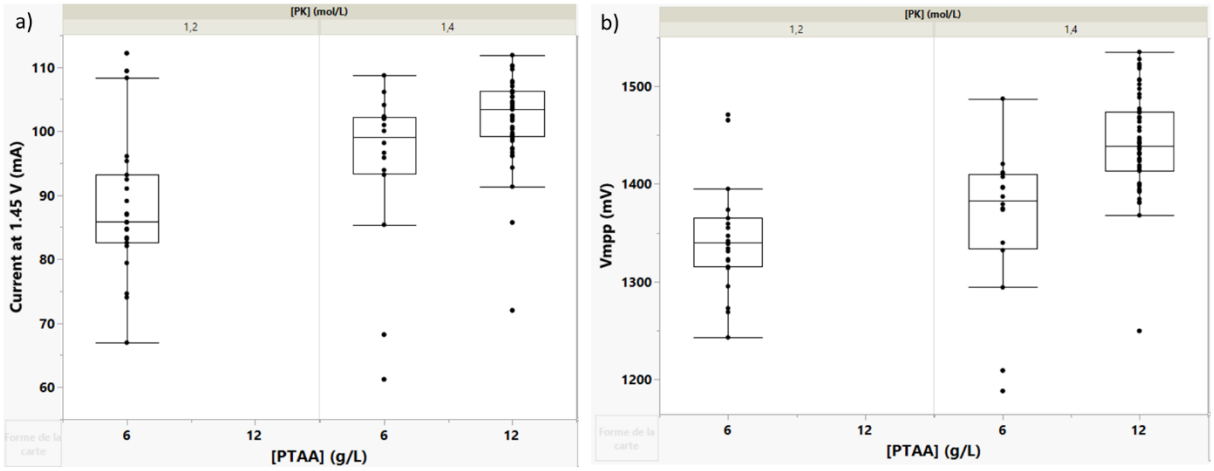

Figure S9 – a) Current delivered at 1.45 V (close to operating point) by the perovskite/silicon tandem solar cells under 1 sun. b) Corresponding maximum power point voltage. Results are shown here for devices before encapsulation.

Performance of the tandem solar cells before and after outdoor ageing in Ispra

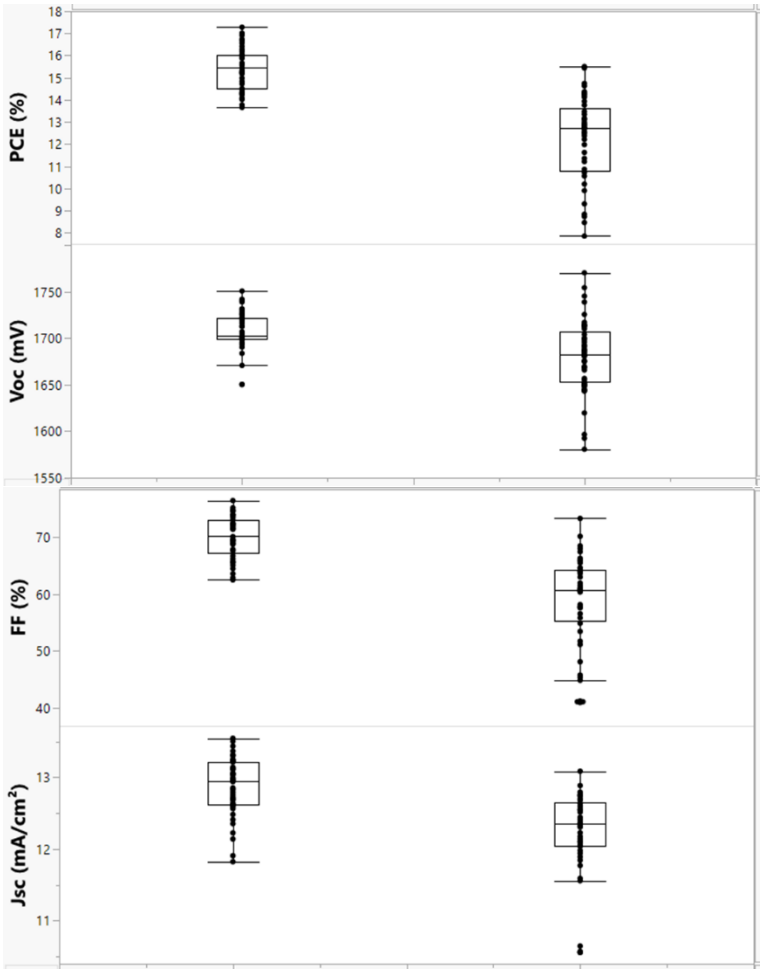

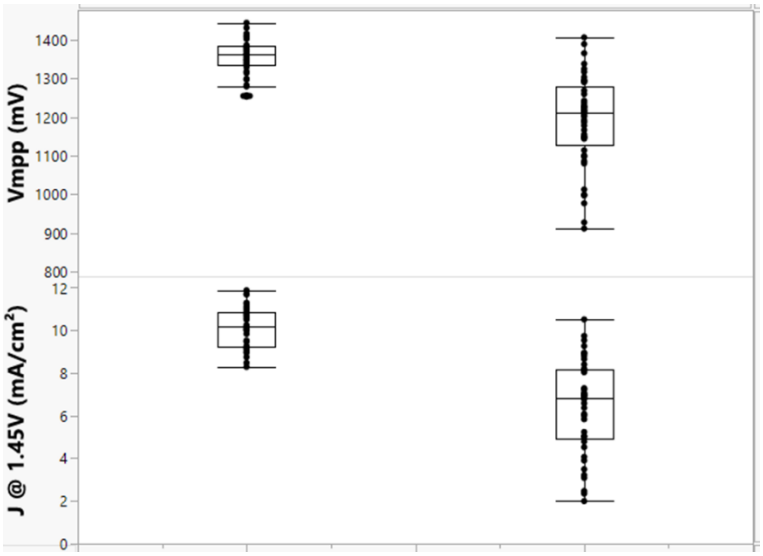

Figure S10 – PV performance parameters of the forty-five perovskite/silicon tandem solar cells before and after outdoor ageing in Ispra, measured under calibrated solar simulator. Power Conversion Efficiency (PCE), open circuit voltage (V_{oc}), fill factor (FF), short circuit current density (J_{sc}), voltage at maximum power point (V_{mpp}) and current density at 1.45 V (J @ 1.45V).

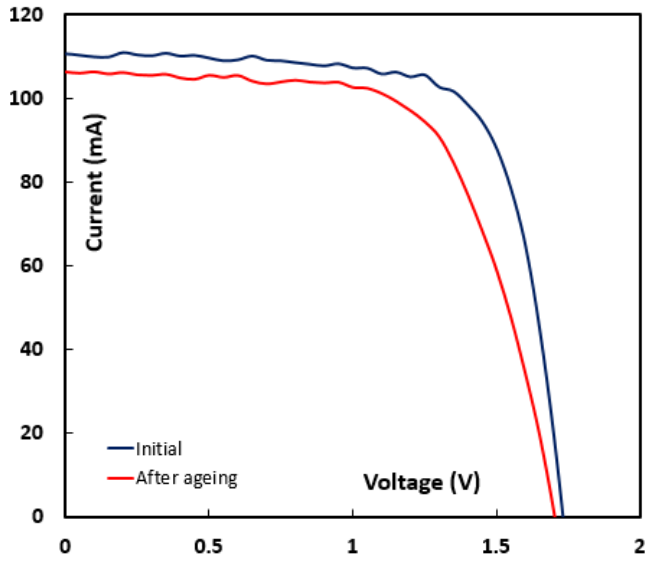

Figure S11 – Typical I(V) curve of a perovskite/silicon tandem solar cell before (in blue) and after ageing (in red).

Details of reports from literature used to build the graphs from Figure 6

Table S6 – Comparison of best IPEC cells and modules from this study with State of Art devices: illuminated or absorber active area, STH efficiency and tested lifetime (results are gathered for various ageing conditions: light cycling, continuous illumination or outdoor).

Device type	Illuminated or active area (cm^2)	STH (%)	Tested lifetime (h)	Ref.
PVE or PEC with III-V multi-junctions	0.2	19	20	Cheng *et al.*(51)
	0.316	31.2	48	Jia *et al.* (56)
	1	14	1000	Kistler *et al.* (57)
	4	17	2	Tembhurne *et al.*(24)
	8	N.A.	96	Kistler *et al.*(10)
	385 000	20.3	~ 5000	Holmes *et al.*(11)
PVE or PEC with perovskite-based multi-junctions	0.1875	17.52	0.1	Park *et al.*(13)
	0.3	17.6	0.1	Karuturi *et al.*(15)
	0.44	20.8	102	Fehr *et al.*(20)
	0.5	21.32	8	Pan *et al.*(18)
	0.5091	19.68	20	Wang *et al.*(17)
	1	17	0.1	Sharma *et al.*(58)
	1	20	15	Wang *et al.*(16)
	1	21.5	72	Datta *et al.*(19)
	1	15	120	Song *et al.*(59)
	1.42	18.7	2.5	Gao *et al.*(14)
	7.6	**8**	**72**	**IPEC cell from this work (Table 1)**
	342	**6.3**	**72**	**IPEC modules from this work (Table 4)**
PVE or PEC with single junction absorbers	100	9.1	100	Pehlivan *et al.*(60)
	100	10	168	Calnan *et al.*(25)
	100	13.4	12	Calnan *et al.*(25)
	2600	7	50	Calnan *et al.*(25)
	100000	10	6500	Lee *et al.*(61)
PC devices	1	0.13	154	Pornrungroj *et al.*(62)
	90 000	0.76	0.5	Nishiyama *et al.*(45)
	1 000 000	0.45	~ 2200	Nishiyama *et al.*(45)

References

55. Honsberg CB, Bowden SG. www.pveducation.org. 2019 [cited 2024 Apr 22]. Solar Radiation on a Tilted Surface. Available from: https://www.pveducation.org/pvcdrom/properties-of-sunlight/solar-radiation-on-a-tilted-surface

56. Jia J, Seitz LC, Benck JD, Huo Y, Chen Y, Ng JWD, et al. Solar water splitting by photovoltaic-electrolysis with a solar-to-hydrogen efficiency over 30%. Nat Commun. 2016 Oct 31;7(1):13237.

57. Kistler TA, Um MY, Agbo P. Stable Photoelectrochemical Hydrogen Evolution for 1000 h at 14% Efficiency in a Monolithic Vapor-fed Device. J Electrochem Soc. 2020 Mar;167(6):066502.

58. Sharma A, Duong T, Liu P, Soo JZ, Yan D, Zhang D, et al. Direct solar to hydrogen conversion enabled by silicon photocathodes with carrier selective passivated contacts. Sustain Energy Fuels. 2022 Jan 18;6(2):349–60.

59. Song Z, Li C, Chen L, Dolia K, Fu S, Sun N, et al. All-Perovskite Tandem Photoelectrodes for Unassisted Solar Hydrogen Production. ACS Energy Lett. 2023 Jun 9;8(6):2611–9.

60. Pehlivan İB, Oscarsson J, Qiu Z, Stolt L, Edoff M, Edvinsson T. NiMoV and NiO-based catalysts for efficient solar-driven water splitting using thermally integrated photovoltaics in a scalable approach. iScience. 2021 Jan 22;24(1):101910.

61. Lee M, Haas S, Smirnov V, Merdzhanova T, Rau U. Scalable Photovoltaic-Electrochemical Cells for Hydrogen Production from Water - Recent Advances. ChemElectroChem. 2022;9(24):e202200838.

62. Pornrungroj C, Mohamad Annuar AB, Wang Q, Rahaman M, Bhattacharjee S, Andrei V, et al. Hybrid photothermal–photocatalyst sheets for solar-driven overall water splitting coupled to water purification. Nat Water. 2023 Nov;1(11):952–60.